UNIVERSITE DE LAUSANNE – FACULTE DE BIOLOGIE ET DE MEDECINE

Institut de Physiologie

Directeur: Professeur Luc Tappy

Hexyl-aminolevulinate mediated photodynamic therapy: how to spare normal urothelium. An in vitro approach.

THESE

Préparée sous la supervision du Professeur honoraire Pavel Kucera
et présentée à la Faculté de biologie et de médecine
de l'Université de Lausanne pour l'obtention du grade de

DOCTEUR EN MEDECINE

Par

Laurent Vaucher

Médecin diplômé de la Confédération Suisse
Originaire de Fleurier, NE

Lausanne

2006

Résumé

Objectifs : La thérapie photodynamique a pour but la destruction sélective du tissu néoplasique par interaction de lumière, d'oxygène et d'une substance photosensibilisatrice (la Protoporphyrine IX dans notre étude). Malgré une accumulation sélective du photosensibilisateur dans le tissu tumoral, la thérapie photodynamique du carcinome urothélial de la vessie peut endommager les cellules normales de l'épithélium urinaire. La prévention de ces lésions est importante pour la régénération de la muqueuse. Notre étude sur un modèle in vitro d'urothélium porcin étudie l'influence de la concentration du photosensibilisateur, des paramètres d'irradiation et de la production d'intermédiaires réactifs de l'oxygène (ROS) sur les effets photodynamique. Le but était de déterminer les conditions seuil pour épargner l'urothélium sain.

Méthode: Dans une chambre de culture transparente à deux compartiments, des muqueuses vésicales de porc maintenues en vie ont été incubées avec une solution d'hexyl-aminolévulinate (HAL), le précurseur de la Protoporphyrine IX. Ces muqueuses ont ensuite été irradiées avec des doses lumineuses croissantes en lumière bleue et en lumière blanche, et les altérations cellulaires ont été évaluées par microscopie électronique à balayage et par un colorant fluorescent, le Sytox green. Nous avons également évalué la production d'intermédiaires réactifs de l'oxygène par la mesure de la fluorescence intracellulaire de Rhodamine 123 (R123), produit de l'oxydation de la Dihydrorhodamine 123 (DHR123) non fluorescente. Ces valeurs ont été corrélées avec celles du photo blanchiment de la PpIX.

Résultats : Le taux de mortalité cellulaire était dépendant de la concentration de PpIX. Après 3 heures d'incubation, la valeur seuil de dose lumineuse pour la lumière bleu était de 0.15 et 0.75 J/cm^2 (irradiance 30 et 75 mW/cm^2, respectivement) et pour

la lumière blanche de 0.55 J/cm^2 (irradiance 30 mW/cm^2). Le taux de photo blanchiment était inversement proportionnel à l'irradiance. Le système de détection des intermédiaires réactifs de l'oxygène DHR123/R123 a démontré une bonne corrélation avec les valeurs seuil pour toutes les conditions d'irradiation utilisées.

Conclusions : Nous avons déterminé les doses lumineuses permettant d'épargner 50% des cellules urothéliales saines. L'utilisation d'une faible irradiance associée à des systèmes permettant de mesurer la production d'intermédiaires réactifs de l'oxygène dans les tissus irradiés pourrait améliorer la dosimétrie in vivo et l'efficacité de la thérapie photodynamique.

Hexyl-aminolevulinate mediated photodynamic therapy: how to spare normal urothelium. An in vitro approach.

Laurent Vaucher MD[1], Patrice Jichlinski MD[3], Norbert Lange PhD[2], Céline Ritter-Schenk[1], Hubert van den Bergh PhD,[4] and Pavel Kucera PhD[1]

[1] Institute of Physiology, University of Lausanne, Switzerland

[2] School of Pharmacy, University of Lausanne, Switzerland

[3] Department of Urology, CHUV Hospital, Lausanne, Switzerland

[4] Swiss Federal Institute of Technology, Lausanne, Switzerland

Running head: conditions sparing normal urothelium in photodynamic therapy

26 pages, 1 table, 5 figures

Key words: urothelium, in vitro, photodynamic lesions, irradiation threshold, dosimetry

Corresponding Author: Laurent Vaucher

Service d'Urologie

Centre Hospitalier Universitaire Vaudois

CH-1011 Lausanne

e-mail: laurent.vaucher@chuv.ch

fax +41 21 3142985

Abstract

Background and Objectives: Photodynamic therapy of superficial bladder cancer may cause damages to the normal surrounding bladder wall. Prevention of these is important for bladder healing. We studied the influence of photosensitizer concentration, irradiation parameters and production of reactive oxygen species (ROS) on the photodynamically induced damage in the porcine urothelium in vitro. The aim was to determine the threshold conditions for the cell survival.

Methods: Living porcine bladder mucosae were incubated with solution of hexylester of 5-aminolevulinic acid (HAL). The mucosae were irradiated with increasing doses and cell alterations were evaluated by scanning electron microscopy and by Sytox green fluorescence. The urothelial survival score was correlated with Protoporphyrin IX (PpIX) photobleaching and intracellular fluorescence of Rhodamine 123 reflecting the ROS production.

Results: The mortality ratio was dependent on PpIX concentration. After 3 hours of incubation, the threshold radiant exposures for blue light were 0.15 and 0.75 J/cm^2 (irradiance 30 and 75 mW/cm^2, respectively) and for white light 0.55 J/cm^2 (irradiance 30 mW/cm^2). Photobleaching rate increased with decreasing irradiance. Interestingly, the DHR123/R123 reporter system correlated well with the threshold exposures under all conditions used.

Conclusions: we have determined radiant exposures sparing half of normal urothelial cells. We propose that the use of low irradiance combined with systems reporting the ROS production in the irradiated tissue could improve the in vivo dosimetry and optimize the PDT.

Introduction

Photodynamic therapy (PDT) is currently approved as an alternative treatment for several benign and malignant diseases such as age related macular degeneration, cutaneous tumors or upper aero-digestive cancers (1) (2). The therapeutic principle relies on a specific light interaction with photosensitized target tissue. A successful outcome depends on numerous variables such as physicochemical, pharmacological and tissue related properties of the photosensitizer (3).

In the case of superficial bladder cancer, the lack of selectivity of the first generation photosensitizers (hematoporphyrin derivatives) and some serious adverse effects, including skin photosensitization and loss of bladder capacity, slowed down the initial enthusiasm for this treatment (4). This was mainly due to the inappropriate localization of the photosensitizing agent in the vessels or in the depth of the bladder wall. Thus, PDT use in urology has remained mainly experimental.

However, photosensitization based on endogenous photoactive protoporphyrin IX (PpIX) synthesized upon topical administration of ALA or ALA derivatives such as hexyl-aminolevulinate (HAL), clearly renewed the interest of PDT development. Topically administered, these derivatives have an excellent specificity for epithelia such as urothelium with a pronounced affinity for tumor tissue. ALA or HAL based fluorescence cystoscopy clearly improves the detection of carcinomas in situ, which are precisely the lesions on which PDT is assumed to be effective (5) (6) (7).

An optimal PDT necessitates considering specific clinical settings and medical indications. While bulky and nodular lesions would suggest the use of red light, penetrating better into deeper tissue layers, in the case of urological superficial tumors, the use of shorter wavelengths (blue light) might be preferential. For practical reasons, the use of white light (containing red component) could be advantageous,

also because powerful light sources are readily available in all urological services performing fluorescence based photodiagnosis.

However, as demonstrated in different animal tumor models, some damage to the normal urothelium may occur during PDT, because normal cells take up the precursors as well (8).

The strong interdependence of irradiance, radiant exposure, photosensitizer concentration and possibly also oxygen availability (ROS precursor) represents a complex scenario for the definition of an optimal photodynamic dose (9). Indeed, it would be extremely difficult to monitor PpIX accumulation or ROS production explicitly under clinical conditions. Alternatively, assuming that the reactions leading to cellular death and to photochemical destruction of the sensitizer are closely coupled, an implicit approach is to monitor the decrease of PpIX fluorescence (PpIX photobleaching) during the PDT and/or ROS appearance in the urothelium.

The present work evaluates the cellular photodamage to porcine urothelium with respect to the photosensitizer concentration and production of reactive oxygen species (ROS). The main objective is to determine irradiation parameters allowing to control the damage to the normal urothelium.

Materials and Methods

Chemicals

5-aminolevulinic acid hexylester hydrochloride (HAL) was synthesized in our laboratory as described previously (10). Solutions of HAL [2 mM] in Tyrode bicarbonate buffer were prepared just prior the use and adjusted to pH 5.3. Rhodamine 101, Na_2HPO_4, NaH_2PO_4, Glutaraldehyde, Dimethylsulfoxide, OsO_4, and Ethanol were purchased from Fluka (Buchs, Switzerland) and used without further

purification. Sytox green and Dihydro-Rhodamine 123 (DHR123) were obtained from molecular probes (Eugene, US). Stock solution of DHR123 in DMSO [1 mM] was conserved at –11°C in the dark and diluted for use with Tyrode bicarbonate buffer to a final concentration of 10 µmol.

Preparation of pig bladder mucosae

Porcine urothelium were prepared and maintained alive according to Marti et al (11): Pig bladders were obtained from slaughtered animals and kept in Tyrode solution at 4°C until use (1-6 hours post excision). The urothelium was micro dissected from underlying tissue and cut into of approximately 7 x 7 mm fragments. These were mounted in a thermostabilized (37°C) transparent culture chamber and placed under a modified epi-fluorescence microscope. The urothelium divided the chamber into epithelial and submucosal compartments. The submucosal compartment was continuously perfused by oxygenated Tyrode solution, the apical one was exposed to the HAL solution (fig. 1).

PpIX microspectrofluorometry

During incubation with HAL, the PpIX accumulation was followed by microspectrofluorometry as described before (11). In brief, the light of a 100W mercury lamp, filtered at 405 ± 5 nm (Eppendorf, Switzerland) was focused (Lens Planfluotar x10, NA 0.30, Leitz, Germany) on a 0.003 cm^2 area of the urothelial surface. The emitted fluorescence passed through a long pass filter (RG610, Schott, Germany) and a continuous interference filter (Veril, Leitz, Germany) and was recorded by EMI S20 photomultiplier tube. The fluorescence intensity was expressed in arbitrary units. In order to correct possible fluctuations in excitation and emission pathways, all measurements of PpIX fluorescence intensity were normalized

according to the signal of a reference solution (Rhodamine 101 in ethanol, [1µM]) at 635 nm. Tissue autofluorescence, measured in mucosae without preincubation with HAL, was shown to be stable and negligible (11).

Determination of Oxygenating Species

In order to measure the intracellular ROS resulting from the illumination, we used the Dihydro-Rhodamine 123 (DHR123)/Rhodamine 123 (R123). The non-fluorescent DHR123 penetrates into the cells and is known to be converted into fluorescent R123 by a broad range of oxygenating species (12). This system shows minimal overlap of its absorption and emission bands with those of PpIX (Figure 2A). After the HAL preincubation, the accumulation of PpIX was determined. The apical compartment of the transparent culture chamber was then washed twice with Tyrode solution and filled for 15 min with 10µM DHR123. The irradiation, i.e., photodynamic "therapy", was performed as described below and the fluorescence intensity of R123 was measured at 525 nm using an excitation wavelength of 484 ± 5 nm. Fig. 2B shows the kinetics of PpIX accumulation until 8 hours of incubation.

Photodynamic "therapy"

The urothelium was irradiated at 4 separate spots through the objective of the microscope. The power density of the irradiating beam was measured with a calibrated power meter (Research Radiometer IL700, International Light, Newbury Port, US). At 405 nm (blue light), the irradiances at the epithelial surface of the filtered Hg lamp were set to 30 mW/cm^2 and 75 mW/cm^2, respectively. White light illumination was provided by an unfiltered Storz D-Light system (spectral range: 350 – 680 nm Storz, Tuttlingen, Germany). The white light was delivered by a liquid light guide through the ocular of the microscope at 30 mW/cm^2 and the urothelial surface

illuminated as described above. In both cases, the spot size was 0.003 cm^2, and care was taken that irradiated area was illuminated homogenously. At each irradiation spot the time of irradiation, i.e. the radiant exposure was progressively increased and the fluorescence intensities of PpIX at 635 nm and R123 at 525 nm were measured and normalized as previously described. Ten mucosae were used for each condition of irradiation.

Tissue damage evaluation

The induced tissue damage was evaluated according to a binary score system (damage - no damage) based on scanning electron microscopy and confirmed by Sytox green, a specific fluorescent probe for cellular death.

Sytox green fluorescence

Before fixation for electron microscopy, ten irradiated preparations were incubated with Sytox green, which penetrates into dead cells exclusively (13). After 30, 60 and 90 min, the Sytox green fluorescence was studied (Fig 3B) with a combination of filters used for Fluorescein isothiocyanate (FITC, excitation at 450-490 nm, emission >515 nm). The urothelium was then re-incubated with control media for two additional hours allowing evaluation of morphological lesions. Without irradiation, no lesions could be seen until 7 hours in mucosae whether incubated or not with HAL (11).

Scanning Electron Microscopy

A "death cell time" interval of 2 hours after irradiation has been defined experimentally, according to the Sytox green and electronic microscopy observations (see above).

After the two additional hours, mucosae were fixed overnight in glutaraldehyde (2% in phosphate buffered saline) and dehydrated through 70%, 80%, 90% and 100% of ethanol. After post-fixation with OsO_4 (1% in phosphate buffered saline), the samples

were freeze dried with a critical point dryer (CPD030, Balzers, Liechtenstein) coated with gold (S150, Sputter coater, Edwards, Zivy, Basel, Switzerland) and studied by SEM (Jed, Tokyo, Japan). Micrographs were recorded on a Kodak Tri-X-Plan (6x7 cm) roll film.

The effect of PDT was judged on the basis of morphological aspect of the irradiated and non-irradiated areas. Each irradiated area was evaluated according to a binary scoring system: score "1" for area showing signs of necrosis (figs.3A, C), score "0" for area without any photodynamic damage (Fig 4A). The radiant exposure inducing sparring of 50% of cases was defined as the threshold exposure for acceptable photodynamic action on normal urothelium.

Statistics

Bilateral t-test was used to evaluate the results of PpIX bleaching and R123 fluorescence. ANOVA was used to evaluate the variations due to incubation period and radiant exposure. P value of 0.05 is taken as criterion of significance.

Results

Accumulation of PpIX in the urothelium

In presence of HAL, porcine urothelium synthesized the PpIX as documented by the characteristic emission peaks at 635 nm and 703 nm following excitation at 405 nm (fig. 2A). The fluorescence intensity-time profile shows a sigmoid-like character (fig.2B): following an initial slow phase, PpIX fluorescence linearly increases with time and then slows down reaching a plateau value after about 8 hours. As described below, the amount of intracellular PpIX critically determines the sensitivity of urothelium to irradiation.

Cell alterations in the urothelium submitted to HAL mediated PDT

Fig. 3 shows scanning electron micrographs of the urothelial surface after 3 hours of exposure to HAL followed by focal irradiations and 2 supplementary hours of incubation in Tyrode solution. No signs of tissular or cellular abnormalities were observed even after 5 hours of incubation with HAL in non-irradiated preparations. Also, no damage was observed following a 5 J/cm^2 irradiation with white or blue light on non-incubated preparations (data not shown).

In urothelia incubated with HAL, focal irradiation with blue light (figs. 3A) and white light (fig.3D) resulted in alterations with distinct morphological characteristics. In all cases, the urothelial damage was strictly limited to the irradiated area and sharply demarcated from the non-irradiated surroundings that remained perfectly normal. At higher resolution, the damaged areas revealed shrunken, broken and perforated cells (fig.3C). Thus, under our conditions, the HAL mediated photo toxicity results in cell necrosis. This was consistently confirmed by fluorescence of Sytox green, which was present exclusively in the irradiated areas (fig.3B). While blue light induced more superficial lesions, white light destroyed all cell layers until the basement membrane. Although the morphology of the lesions was strongly dependent on the used light source and dose, any combination of illumination parameters led to very reproducible results.

Threshold irradiation doses in the normal urothelium

The outcome of urothelial irradiation has been defined as the fraction of spots damaged by the light. The conditions leading to the cell death in 50% of irradiations were defined as threshold value to spare normal urothelium. The survival or necrosis upon irradiation depends in our conditions on 4 parameters, namely, intracellular PpIX content, wavelength used, irradiance and time of irradiation (the product of the

latter two determines the radiant exposure). The influence of the different factors is documented in fig.4 and table 1.

Fig.4 shows the mortality obtained upon illumination with blue light (75 mW/cm^2) and with respect to the time of incubation (see fig.2B for corresponding PpIX intracellular accumulation). After 1 hour of incubation with HAL, no deleterious effects were noticed with a radiant exposure below 0.3 J/cm^2 and an exposure as high as 3 J/cm^2 had to be used to induce 100% cell mortality. After 4 hours of incubation with HAL, urothelial destruction was observed already at 4 times lower value, about 0.75 J/cm^2. Most importantly, the use of 0.3 - 0.75 J/cm^2 after 2-3 hours of incubation led to the desired threshold, i.e., half dead - half intact cells situation. The variations of mortality ratio due to the incubation time (PpIX accumulation) and radiant exposure are highly significant ($P<0.02$ and $P<0.003$ respectively, Anova).

Table 1 shows the results obtained with preparations incubated for 3 hours, which represents a clinically acceptable intravesical instillation time. It shows that the highest threshold value was observed with 405 nm and 75 mW/cm^2 and the lowest for the same wavelength at 30 mW/cm^2. For the white light irradiation at 30 mW/cm^2, an intermediate threshold value was found. For identical irradiance, the threshold value for white light irradiation was 3.7 times higher than for blue light irradiation.

PpIX photobleaching and ROS production

Assuming that the reactions leading to cellular death and to photochemical destruction of the sensitizer are closely related, we monitored the decrease of PpIX fluorescence (PpIX photobleaching) and ROS appearance in the urothelium during the PDT.

This was done in urothelium preincubated for 3 hours and irradiated under conditions identical to those used to establish the threshold values, i.e., 30 and 75 mW/cm^2 for blue light and 30 mW/cm^2 for the white light.

Fig.5 shows that, under strictly identical experimental conditions, the kinetics of PpIX photobleaching and the ROS generation were quasi mirror symmetrical and very reproducible. The photobleaching followed a double exponential function and doses that led to decrease of initial PpIX fluorescence intensity by 1/e value were for the blue light 0.37 J/cm^2 at 30 mW/ cm^2 and 0.68 J/cm^2 at 75 mW/cm^2. Under white light, the corresponding bleaching radiant exposure was 2.2 J/cm^2 at 30 mW/cm^2. The increase in fluorescence of R123 with increasing radiant exposure was also fitted according to a sum of two exponential terms. Most interestingly, for the 3 irradiation conditions, the total normalized accumulated amount of R123 was the same at the corresponding threshold values (table 1). Furthermore, for moderate irradiance, i.e. 30 mW/cm^2, the photobleaching data correlated linearly with the R123 intensities (fig.5 inserts).

The threshold values for radiant exposure were correlated with PpIX photobleaching and R123 accumulation curves for each condition of irradiation (Fig 5).

Discussion

Urothelial destruction

Although tissue photodestruction may result from apoptosis or necrosis (14), the mechanisms leading to cell death in the case of HAL mediated PDT presented here were mainly due to necrosis. This conclusion, based on scanning electron microscopy, was confirmed by the use of Sytox Green known to emit a green fluorescence upon penetration in necrotic cells exclusively. We did not use tissue

viability test, as it was already done previously (11). We cannot extrapolate from this experiment the prevailing cell death mechanism (apoptosis versus necrosis) in clinical use. Although our observations demonstrate necrosis, other studies show the importance of apoptosis (15) (16).

An observation which might be of interest in PDT strategies in urology is that white light irradiation resulted in the destruction and "washout" of the complete urothelial layer until the basement membrane. On the contrary, using blue light destroyed only superficial layers.

Sparing of the normal urothelium

An optimal result of photodynamic therapy would be a complete disappearance of tumour areas with a preserved benign surrounding tissue facilitating the healing process. Therefore, determination of PDT conditions sparing the normal urothelium is of major concern.

For identical irradiances the threshold value for white light irradiation was 3.7 times higher than for blue light irradiation. By folding the excitation spectra of the both light sources with the absorption spectra of PpIX in vitro, one can estimate a relative number of absorbed photons for both cases. In our case, about 2.8 times more photons are absorbed when using blue light instead of white light at the same photon density. Assuming that the total number of absorbed photons represents a measure of produced oxygenating species and that the absorption spectrum of PpIX does not change considerably in the cell microenvironment, the small difference by a factor 1.3 (3.7/2.8) could be explained by the formation of photoproducts during PDT.

Fragmentation of the tetrapyrrolic structure has been shown to result in a blue shift of the absorption spectra (17). However, when the tetrapyrrolic stem structure remains

intact the main photoproducts of PpIX formed by PDT in vitro have an excitation maximum at 450 nm (18). Furthermore, new bands in the far-red region of the spectrum will appear. In general, such photoproducts are also photodynamically active and due to their different absorption characteristics will contribute more to the phototoxicity under white than under blue irradiation. No specific analysis of the different photoproducts in blue or in white light illumination was performed.

Finally, the threshold values decreased with decreasing irradiance. This observation is in agreement with a number of other studies that have reported an enhancement of photodynamic damage with decreasing irradiance (19) (20) (21).

The presented results show that the threshold value for healthy cells depends on a compromise between the PpIX concentration and the used radiant exposure. For an optimized PDT, it will be attractive to keep the PpIX concentration in normal cells at a sub critical level or to use a radiant exposure that enables to preserve the tissue for a given concentration. For example, reduction of incubation time from 4 to 2 hours may spare about a half of the urothelium irradiated at 0.75J/cm^2. Furthermore, one could conclude from these experiments that, for tumor cells that have accumulated PpIX about 5 times more than normal cells (which in urology is the case for carcinoma in situ), one could apply 4 times weaker radiant exposure in order to destroy the tumors while keeping the healthy tissue intact. As shown in fig.4, at 405 nm radiant exposure of 3 J/cm^2 destroyed effectively the PpIX loaded urothelium under all conditions studied. Using 5-ALA given intravenously, Grönland-Pakkanen et al. (22) have shown that superficial bladder damage can be observed in healthy rats urothelium with radiant exposures of 20-40 J/cm2 with light at 635 nm, while 80 J/cm2 showed full thickness damage. Therefore, they have proposed to use the latter for the destruction of CIS. However, as shown by van Staveren et al.(23), PDT induced tissue damages

can vary according to the route of administration. In their studies, radiant exposures of 100 J/cm2 at 635 nm induced irreversible damage to pig bladder walls in vivo, when solutions of 5-ALA were applied intravesically at 300mM. Similar conditions were used by another group (24) showing that selective damage to chemically induced bladder tumors can be achieved without destroying the normal urothelium.

Photobleaching monitoring and ROS reporter system

An approach to perform implicit dosimetry consists of monitoring the decrease of photosensitizer fluorescence intensity caused by photobleaching. Basically, this approach assumes that the same reactions leading to cellular death following PDT are similarly involved in the photochemical destruction of the photosensitizer. The possibility of using photobleaching to monitor dosimetry during PDT had been subject of numerous studies and an extensive review on this subject has recently been reviewed by Wilson et al (25). However, to establish the relationship among the photobleaching, the therapeutically active species and the final treatment outcome remains a challenge. Only a few studies have focused specifically on the correlation of the above-mentioned photosensitizer depletion and the resulting photodynamic response of tissue (19, 26-28). In order to test the hypothesis that photobleaching measurements can be used to optimize HAL-mediated PDT of superficial bladder cancer, we have pre-incubated pig bladder mucosae with HAL during three hours and measured the decrease of PpIX fluorescence intensity during PDT. Under these conditions, the PpIX fluorescence intensity - time profiles cannot be described by a simple exponential function of the radiant exposure and consequently photobleaching is not a simple first order process. The traces in fig. 5 represent the weighted non-linear least square fits of the data using a sum of two exponential terms. In contrast to recent findings of Robinson et al. (19) in hairless mice and of Georgakoudi et al.

(29) in vitro, a double exponential decay fitted our photobleaching curves better than fitting according to a second order process. Also, Moan et al. (30) described the PpIX decay during PDT in vitro by a sum of two exponential terms, which is in agreement with our study. These authors ascribed this characteristic to the relocation of the photosensitizer during PDT or its chemical modification that contributes to the photobleaching process. Furthermore, different photobleaching processes of protein bound and unbound photosensitizers have been proposed.

Nevertheless, our data show that the rate of photobleaching significantly increases with decreasing irradiance. Since the oxygen supply is one of the limiting factors in PDT, this phenomenon could result from a too high initial oxygen consumption imposed by a high irradiance. This hypothesis is in agreement with the data and calculations of Foster's group (31,32).

Thus, in vitro, where the initial amount of PpIX can be measured, photobleaching monitoring at lower irradiance can be used for dosimetry. In clinical situations, however, relative rather than absolute amounts of bleached PpIX would be measured. In addition, the fraction of depleted PpIX to induce cell death could be smaller than the interindividual variations of PpIX accumulation. Technically, this observation entails a further challenge, since it implies a rather exact assessment of small changes against a large background signal having the same optical properties. However, the use of other methods for the determination of therapeutic outcomes might become important, when the measured amount of photosensitizer cannot be directly correlated with the tissular response, as very recently demonstrated by El Khatib et al. (33)

Besides monitoring of photobleaching for dosimetry purposes, other implicit methods, such as measuring the photosensitizer triplet state, triplet state lifetimes and use of

measurable changes in tissue or environmental fluorescence reporter molecules, have rarely been exploited. We have adopted an interesting alternative, i.e., monitoring of R123 fluorescence intensity, which reflects the total amount of oxygenating species produced during irradiation. In these experiments, the fluorescence intensity of R123 increased with increasing radiant exposure. Most remarkably, for the three irradiation conditions used, the total normalized accumulated amount of R123 was the same at the corresponding threshold values (see Table 1). Furthermore, at 30 mW/cm^2, the R123 kinetics correlates linearly with the photobleaching data, which again supports the idea of using low irradiances. Due to the induction of R123 during PDT there might be an additional effect from R123 induced $^1O_2$ during irradiation with white light. Since, extinction coefficient of R123 is only small at 405 nm, only minimal photodamage can be assumed under blue light irradiation. However, R123 is known to be a relatively weak phototoxin (34) and at the concentration of DHR123 used here, the production of ROS resulting by the above mentioned reaction should be negligible.

The introduction of a reporter system such as DHR123/R123 into PDT procedure would be very useful for the following reasons: a) the total intensity of R123 can be used as direct criterion of the delivered photodynamic dose and, b) the correlation of R123 fluorescence intensity with PpIX photobleaching helps to optimize the irradiance related to the available oxygen concentration. Nevertheless, in this study, this ROS reporting system was only used after 3 hours incubation of HAL. Therefore we cannot extrapolate what would have been the results according to different incubation conditions, which play a role in subcellular PpIX localization.

However, although toxicity and metabolism of R123 at higher doses has been evaluated (35), no human toxicological studies exist on the reporting system

DHR123/R123 at the concentration we used in our study. Alternatively, other fluorescent reporter systems, known for their sensitivity towards ROS species, such as dichlorodihydrofluorescein diacetate and its analogs of dihydrorhodamine 6G, might be of potential interest. Although a direct extrapolation to the real in vivo situation is not possible for the time being, such extrapolation would imply that the R123 activation would be similar to the cell kill kinetics. This would require similar subcellular localization (which might vary for PpIX between 1 and 4 hours post incubation) and also similar contributions of singlet oxygen and other ROS to the R123 activation and cell kill, respectively. However, the present study shows, for the first time, the feasibility to use such ROS reporter systems to monitor a photodynamic action during PDT by simple fluorescence imaging.

Conclusions

For an optimal photodynamic therapy, the determination of conditions sparing the normal urothelium facilitating the healing process is of major concern. The in vitro preparation of the porcine mucosa preincubated with HAL allowed us to determine incubation condition for photodetection in clinics. We also correlated the extent of tissue damage with the intracellular PpIX concentration, irradiations wavelength and irradiance and with the reactive oxygen species produced upon irradiation.

Under moderate irradiances, photobleaching was found to be a good predictor of tissue damage and only a small fraction (10-20%) of PpIX had to be destroyed in order to induce cell death. In addition, the DHR123/R123 reporter system was well correlated with the threshold exposures under all conditions used.

We propose that the use of low irradiances combined with systems reporting the ROS production in the irradiated tissue could improve the in vivo dosimetry and

optimize the PDT of the superficial bladder carcinoma. Clinical studies are however warranted.

Acknowledgements

This work was supported by the Swiss National Science Foundation (grant 3200-056050.98 to P.J. and P.K.) and the Schering Research Foundation (grant to N.L.)

References

1. Brown SB, Brown EA, Walker I. The present and future role of photodynamic therapy in cancer treatment. Lancet Oncol 2004; 5(8):497-508.
2. Michels S, Schmidt-Erfurth U. Photodynamic therapy with verteporfin: A new treatment in ophthalmology. Semin Ophthalmol 2001; 16(4):201-206.
3. Solban N, Ortel B, Pogue B, Hasan T. Targeted optical imaging and photodynamic therapy. Ernst Schering Res Found Workshop 2005(49):229-258.
4. Jichlinski P, Leisinger HJ. Photodynamic therapy in superficial bladder cancer: past, present and future. Urol Res 2001; 29(6):396-405.
5. Jichlinski P, Guillou L, Karlsen SJ, Malmstrom PU, Jocham D, Brennhovd B, Johansson E, Gartner T, Lange N, van den Bergh H, Leisinger HJ. Hexyl aminolevulinate fluorescence cystoscopy: new diagnostic tool for photodiagnosis of superficial bladder cancer--a multicenter study. J Urol 2003; 170(1):226-229.
6. Lange N, Jichlinski P, Zellweger M, Forrer M, Marti A, Guillou L, Kucera P, Wagnieres G, van den Bergh H. Photodetection of early human bladder cancer based on the fluorescence of 5-aminolaevulinic acid hexylester-induced protoporphyrin IX: a pilot study. Br J Cancer 1999; 80(1-2):185-193.
7. Jocham D, Witjes F, Wagner S, Zeylemaker B, van Moorselaar J, Grimm MO, Muschter R, Popken G, Konig F, Knuchel R, Kurth KH. Improved detection and treatment of bladder cancer using hexaminolevulinate imaging: a prospective, phase III multicenter study. J Urol 2005; 174(3):862-866; discussion 866.
8. Kamuhabwa AA, Roskams T, D'Hallewin MA, Baert L, Van Poppel H, de Witte PA. Whole bladder wall photodynamic therapy of transitional cell carcinoma rat bladder tumors using intravesically administered hypericin. Int J Cancer 2003; 107(3):460-467.
9. van den Bergh H. On the evolution of some endoscopic light delivery systems for photodynamic therapy. Endoscopy 1998; 30(4):392-407.
10. Lange N, Vaucher L, Marti A, Etter AL, Gerber P, van Den Bergh H, Jichlinski P, Kucera P. Routine experimental system for defining conditions used in photodynamic therapy and fluorescence photodetection of (non-) neoplastic epithelia. J Biomed Opt 2001; 6(2):151-159.
11. Marti A, Lange N, van den Bergh H, Sedmera D, Jichlinski P, Kucera P. Optimisation of the formation and distribution of protoporphyrin IX in the urothelium: an in vitro approach. J Urol 1999; 162(2):546-552.
12. Emmendorffer A, Hecht M, Lohmann-Matthes ML, Roesler J. A fast and easy method to determine the production of reactive oxygen intermediates by human and murine phagocytes using dihydrorhodamine 123. J Immunol Methods 1990; 131(2):269-275.
13. Gaforio JJ, Serrano MJ, Ortega E, Algarra I, Alvarez de Cienfuegos G. Use of SYTOX green dye in the flow cytometric analysis of bacterial phagocytosis. Cytometry 2002; 48(2):93-96.
14. Marcinkowska A, Malarska A, Saczko J, Chwilkowska A, Wysocka T, Drag-Zalesinska M, Wysocka T, Banas T. Photofrin--factor of photodynamic therapy induces apoptosis and necrosis. Folia Histochem Cytobiol 2001; 39 Suppl 2:177-178.

15. Kuzelova K, Grebenova D, Pluskalova M, Marinov I, Hrkal Z. Early apoptotic features of K562 cell death induced by 5-aminolaevulinic acid-based photodynamic therapy. J Photochem Photobiol B 2004; 73(1-2):67-78.
16. Luksiene Z, Eggen I, Moan J, Nesland JM, Peng Q. Evaluation of protoporphyrin IX production, phototoxicity and cell death pathway induced by hexylester of 5-aminolevulinic acid in Reh and HPB-ALL cells. Cancer Lett 2001; 169(1):33-39.
17. Rotomskis R, Bagdonas S, Streckyte G. Spectroscopic studies of photobleaching and photoproduct formation of porphyrins used in tumour therapy. J Photochem Photobiol B 1996; 33(1):61-67.
18. Bagdonas S, Ma LW, Iani V, Rotomskis R, Juzenas P, Moan J. Phototransformations of 5-aminolevulinic acid-induced protoporphyrin IX in vitro: a spectroscopic study. Photochem Photobiol 2000; 72(2):186-192.
19. Robinson DJ, de Bruijn HS, van der Veen N, Stringer MR, Brown SB, Star WM. Fluorescence photobleaching of ALA-induced protoporphyrin IX during photodynamic therapy of normal hairless mouse skin: the effect of radiant exposure and irradiance and the resulting biological effect. Photochem Photobiol 1998; 67(1):140-149.
20. Hua Z, Gibson SL, Foster TH, Hilf R. Effectiveness of delta-aminolevulinic acid-induced protoporphyrin as a photosensitizer for photodynamic therapy in vivo. Cancer Res 1995; 55(8):1723-1731.
21. Veenhuizen RB, Stewart FA. The importance of fluence rate in photodynamic therapy: is there a parallel with ionizing radiation dose-rate effects? Radiother Oncol 1995; 37(2):131-135.
22. Gronlund-Pakkanen S, Pakkanen TM, Talja M, Kosma VM, Ala-Opas M, Alhava E. The morphological changes in rat bladder after photodynamic therapy with 5-aminolaevulinic acid-induced protoporphyrin IX. BJU Int 2000; 86(1):126-132.
23. Van Staveren HJ, Beek JF, Verlaan CW, Edixhoven A, De Reijke TM, Brutel De La Rivi EG, Star WM. Comparison of normal piglet bladder damage after PDT with oral or intravesical administration of ALA. Lasers Med Sci 2002; 17(4):238-245.
24. Kriegmair M, Waidelich R, Lumper W, Ehsan A, Baumgartner R, Hofstetter A. Integral photodynamic treatment of refractory superficial bladder cancer [see comments]. J Urol 1995; 154(4):1339-1341.
25. Wilson BC, Paterson MS, Lilge L. Implicit and explicit dosimetry in photodynamic therapy: a new paradigm. Lasers Med Sci 1997; 12:182-.
26. Robinson DJ, de Bruijn HS, van der Veen N, Stringer MR, Brown SB, Star WM. Protoporphyrin IX fluorescence photobleaching during ALA-mediated photodynamic therapy of UVB-induced tumors in hairless mouse skin. Photochem Photobiol 1999; 69(1):61-70.
27. Glanzmann T, Forrer M, Blant SA, Woodtli A, Grosjean P, Braichotte D, van den Bergh H, Monnier P, Wagnieres G. Pharmacokinetics and pharmacodynamics of tetra(m-hydroxyphenyl)chlorin in the hamster cheek pouch tumor model: comparison with clinical measurements. J Photochem Photobiol B 2000; 57(1):22-32.
28. Rhodes LE, Tsoukas MM, Anderson RR, Kollias N. Iontophoretic delivery of ALA provides a quantitative model for ALA pharmacokinetics and PpIX phototoxicity in human skin. J Invest Dermatol 1997; 108(1):87-91.

29. Georgakoudi I, Foster TH. Singlet oxygen- versus nonsinglet oxygen-mediated mechanisms of sensitizer photobleaching and their effects on photodynamic dosimetry. Photochem Photobiol 1998; 67(6):612-625.
30. Moan J, Streckyte G, Bagdonas S, Bech O, Berg K. Photobleaching of protoporphyrin IX in cells incubated with 5-aminolevulinic acid. Int J Cancer 1997; 70(1):90-97.
31. Mitra S, Finlay JC, McNeill D, Conover DL, Foster TH. Photochemical oxygen consumption, oxygen evolution and spectral changes during UVA irradiation of EMT6 spheroids. Photochem Photobiol 2001; 73(6):703-708.
32. Coutier S, Mitra S, Bezdetnaya LN, Parache RM, Georgakoudi I, Foster TH, Guillemin F. Effects of fluence rate on cell survival and photobleaching in meta-tetra-(hydroxyphenyl)chlorin-photosensitized Colo 26 multicell tumor spheroids. Photochem Photobiol 2001; 73(3):297-303.
33. El Khatib S, Didelon J, Leroux A, Bezdetnaya L, Notter D, D'Hallewin M. Kinetics, biodistribution and therapeutic efficacy of hexylester 5-aminolevulinate induced photodynamic therapy in an orthotopic rat bladder tumor model. J Urol 2004; 172(5 Pt 1):2013-2017.
34. Martin OC, Pagano RE. Internalization and sorting of a fluorescent analogue of glucosylceramide to the Golgi apparatus of human skin fibroblasts: utilization of endocytic and nonendocytic transport mechanisms. J Cell Biol 1994; 125(4):769-781.
35. Castro DJ, Gaskin A, Saxton RE, Reisler E, Nishimura E, To SY, Rodgerson DO, Layfield LJ, Tartell PB, et al. Photodynamic therapy using rhodamine-123 as a new laser dye: biodistribution, metabolism and histology in New Zealand rabbits. Laryngoscope 1991; 101(2):158-164.

Legends to tables and figures

Table 1: Outcome of irradiation of the PpIX loaded normal porcine urothelium

Threshold values correspond to irradiation doses resulting in 50% of damaged spots. The normalized fluorescence intensity (arbitrary units) of R123 reflects the total reactive oxygen species generated in the illuminated cells. Interestingly, this value is the same whatever the irradiation conditions. Three hours of incubation with HAL. Ten mucosae per condition.

Figure 1: Thermostabilized (37°C) transparent culture chamber placed under a modified epi-fluorescence microscope. The urothelium divided the chamber into epithelial and submucosal compartments. The submucosal compartment was continuously perfused by an oxygenated Tyrode solution, the apical one was exposed to the HAL and DHR123 solution.

Figure 2: Spectral analysis of PpIX and Rhodamine 123, and accumulation of PpIX in the normal urothelium

A: Spectral analysis of the excitation and emission fluorescence of PpIX and R123. Note the minimal overlap of R123 absorption and emission bands with those of PpIX.

B: Fluorescence intensity (arbitrary units) is proportional to the PpIX accumulated in the urothelial cells and increases during the incubation with 2 mM HAL. Excitation at 405 nm, emission measured at 635 nm.

Figure 3: Evaluation of the urothelial damage upon irradiation with blue and white light

A: Scanning electron micrograph showing a necrotic lesion of superficial and deeper cells. The lesion is strictly confined to the irradiated area (405 nm, irradiance 75 mW/cm^2, dose 5 J/cm^2). **B:** The same preparation as in A was stained prior the fixation with Sytox green, which upon penetration into dead cells becomes fluorescent. **C:** Shrunken and perforated cell after irradiation as compared to non irradiated urothélium with intact umbrella cells. **D:** Lesion concerning all the urothelial cell layers. The majority of dead cells were washed out but some remaining dead cells adhere to an intact basement membrane. Notice again the normal aspect of the non-irradiated surrounding urothelium (white light, irradiance 30 mW/cm^2, dose 2 J/cm^2). Incubation with HAL for 3 hours, fixation 2 hours after irradiation

Figure 4: Influence of irradiation parameters and incubation time on the fate of irradiated urothelial cells

The cell death is defined as the fraction of spots damaged by the light. The 0.5 level indicates the threshold conditions. **A:** After 2 hours of incubation, the threshold value is between 0.3 and 0.75 J/cm^2. Ten mucosae per condition, incubation with HAL, irradiation with 405 nm light at an irradiance of 75 mW/cm^2. **B:** Variation of incubation with HAL (i.e. PpIX concentration) and radiant exposure. Ten mucosae per condition. Irradiation with 405 nm light at an irradiance of 75 mW/cm^2.

Figure 5: Influence of the light dose on PpIX bleaching and cell R123 accumulation

PpIX bleaching [squares], cell accumulation of R123 [circles]. **A:** blue light, 75 mW/cm^2. **B**: blue light, 30 mW/cm^2. **C:** white light, 30 mW/cm^2. The curves represent weighted non-linear least square fits of the data using a sum of two exponential terms. The bleaching and R123 levels corresponding to threshold doses (see table 1) are shown in black symbols. The inserts in B and C indicate that, at low irradiance and equivalent doses, there is a good correlation between the relative amount of the bleached PpIX and the cell R123 fluorescence. Ten mucosae per condition.

Table 1: Outcome of irradiation of the PpIX loaded normal porcine urothelium

Irradiation Conditions	Estimated threshold [J/cm^2]	Fraction of bleached PpIX	Mean Normalized R123 fluorescence [a.u.]
Blue Light [75mW/cm^2]	0.75	0.41±0.10	0.14±0.05
		p<0.05	
Blue Light [30mW/cm^2]	0.15	p<0.01 0.18±0.15	0.14±0.17
		p<0.1	
White Light [30mW/cm^2]	0.55	0.11±0.09	0.14±0.05

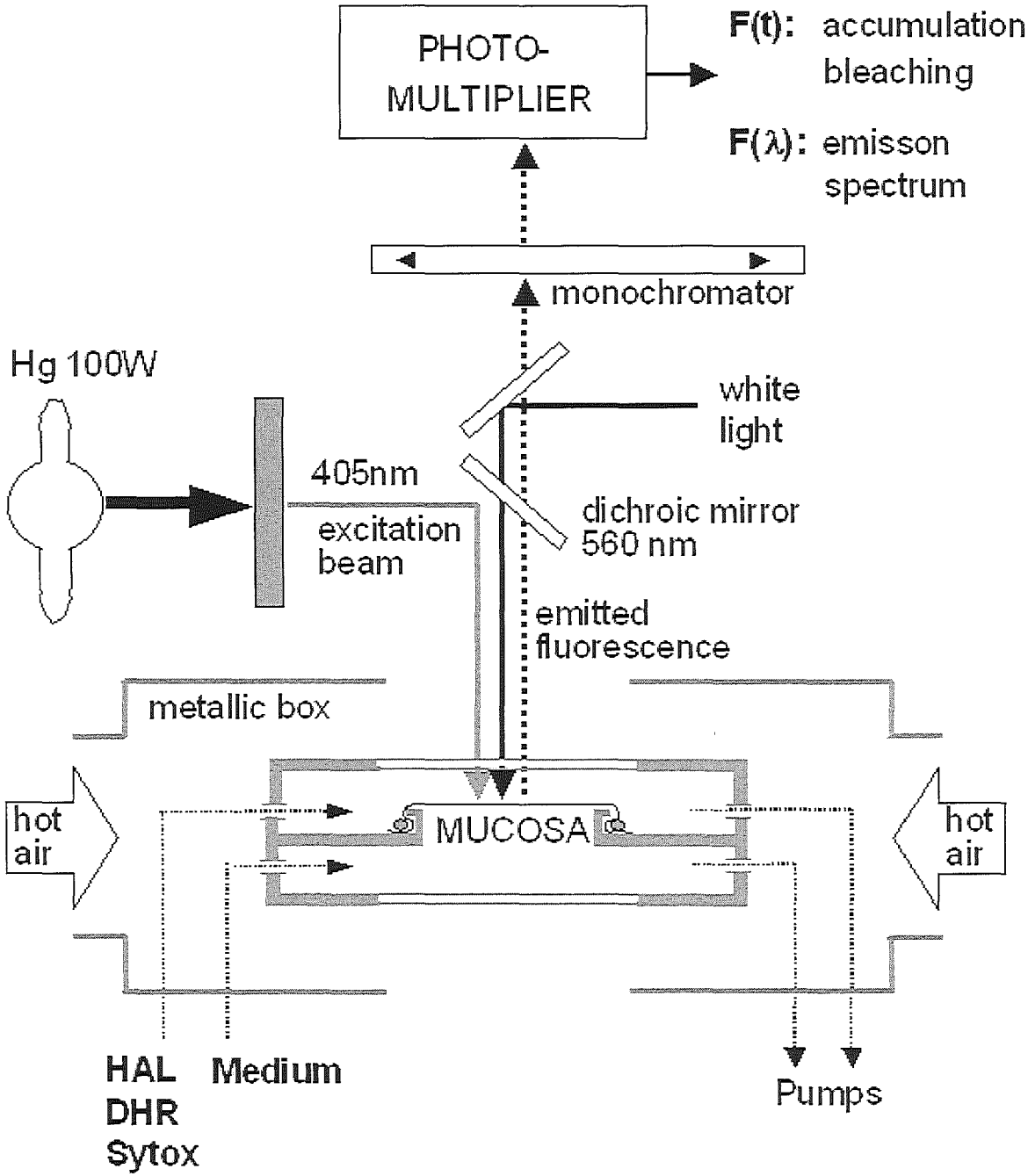

Vaucher & al. Fig.1

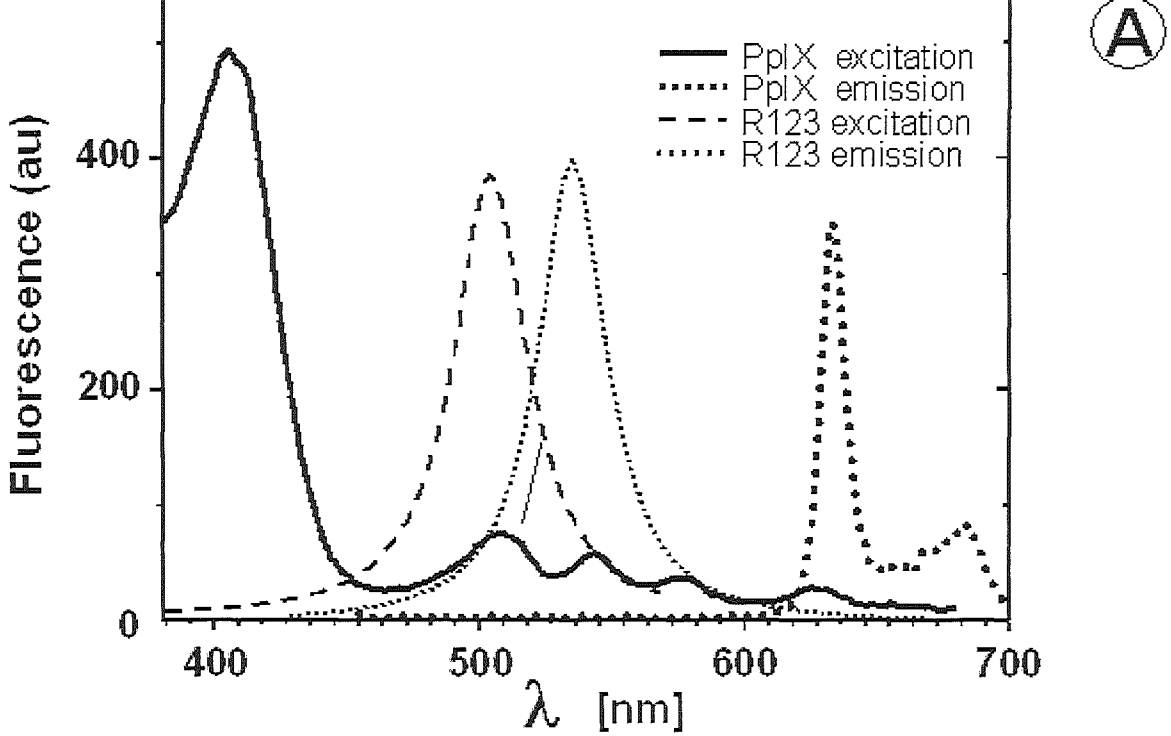

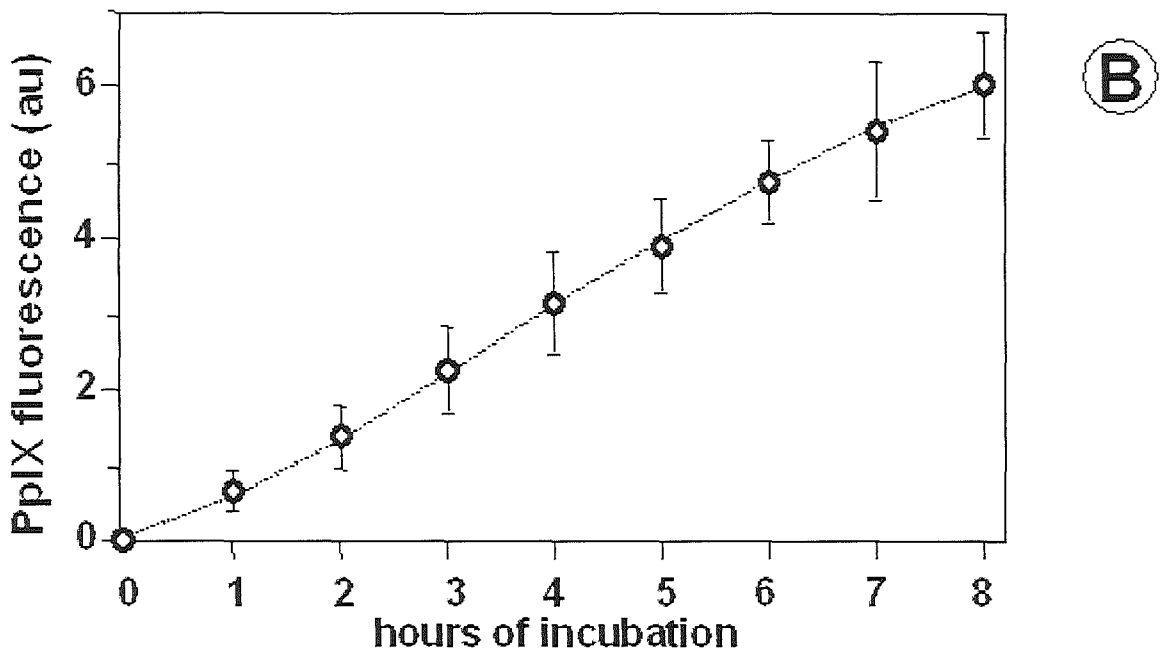

Vaucher & al. Fig.2

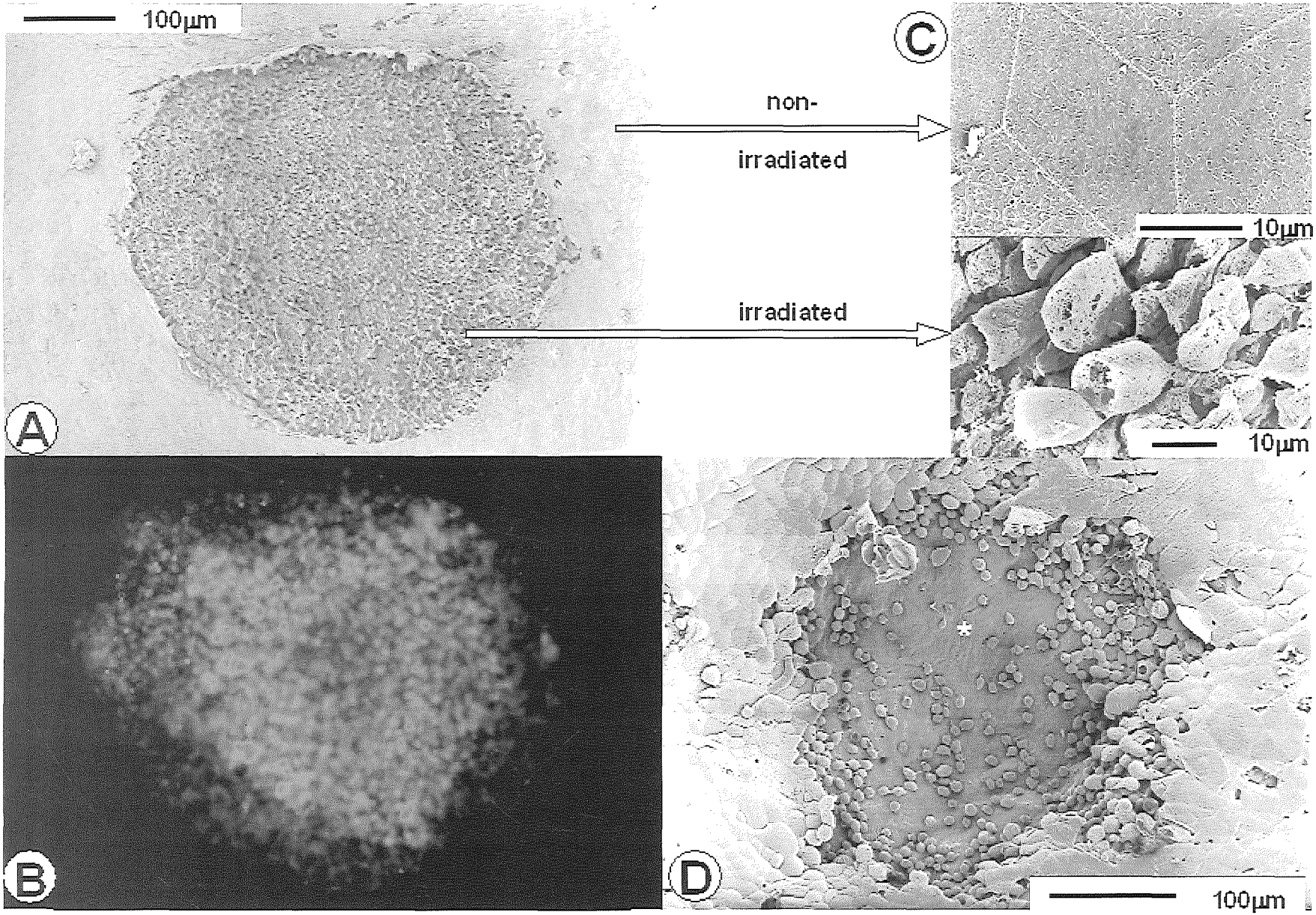

Vaucher & al. Fig.3

A

radiant exposure

Sample	0.3 J/cm²	0.75 J/cm²	1.5 J/cm²	3 J/cm²
1	0	0	0	1
2	0	0	1	1
3	0	0	1	1
4	0	1	1	1
5	0	1	1	1
6	0	1	1	1
7	0	1	1	1
8	0	1	1	1
9	1	1	1	1
10	1	1	1	1

3 hours of incubation

B

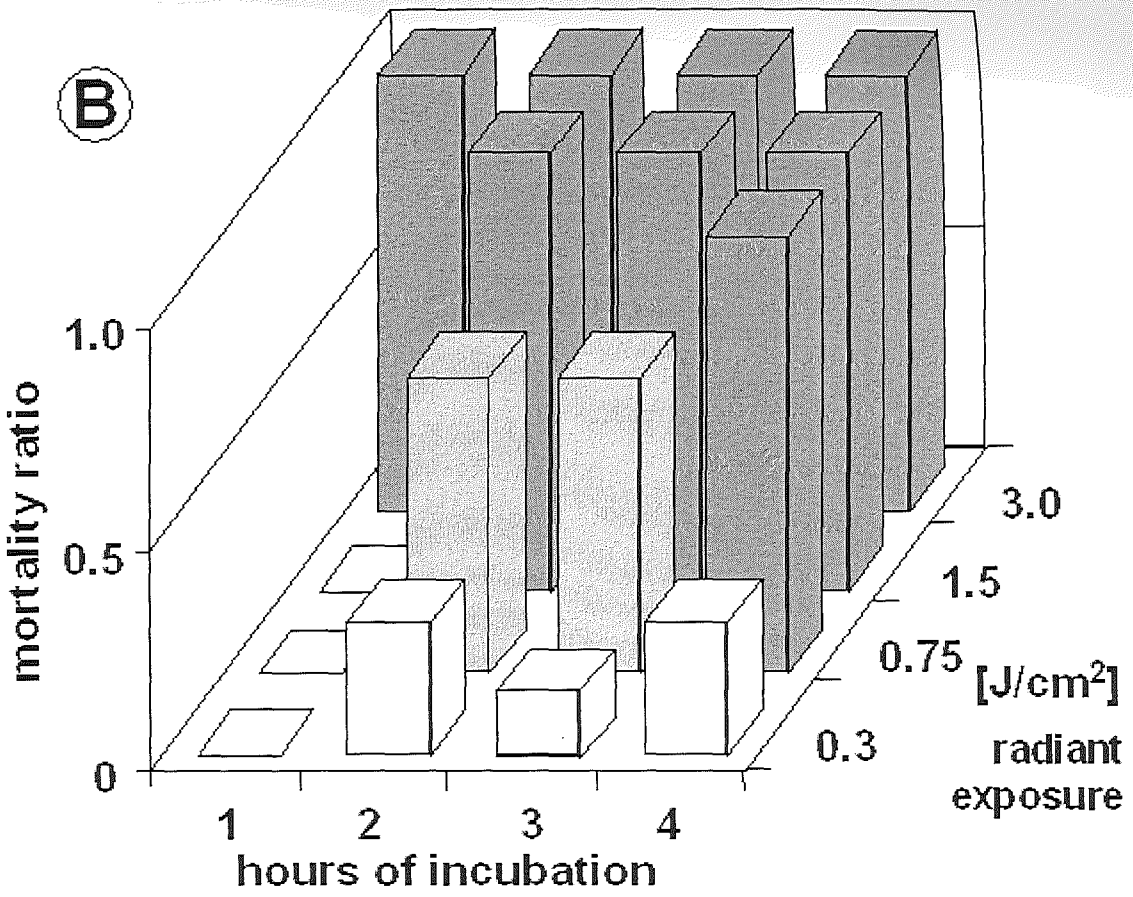

Voucher & al. Fig 4

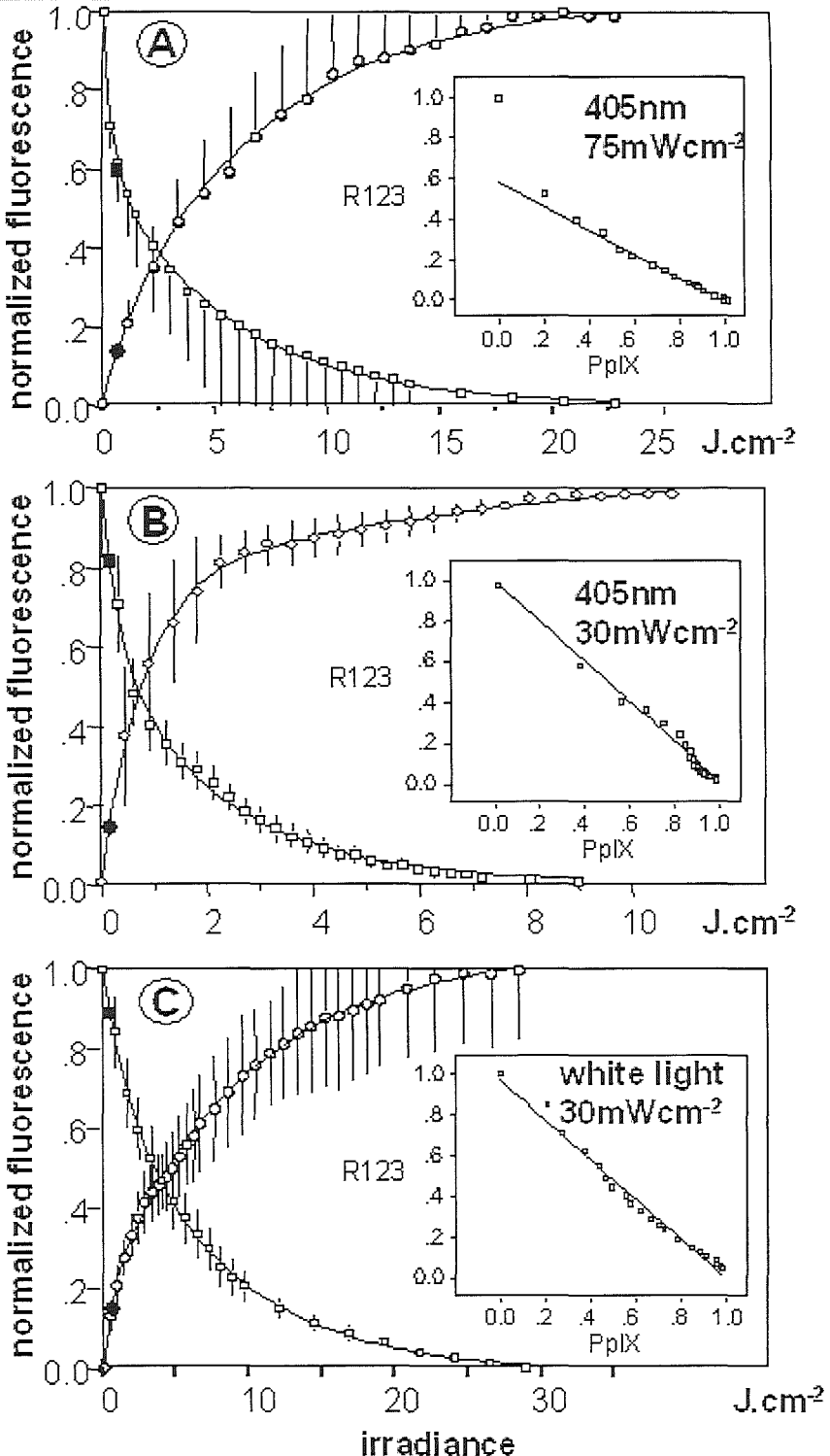

Vaucher & al. Fig.5